DEVELOPMENT OF A THREE-DIMENSIONAL MOMENTUM SOURCE MODEL FOR WIRE-WRAPPED ROD BUNDLES

Rui Hu and Thomas H. Fanning
Argonne National Laboratory, 9700 S. Cass Avenue, Argonne, IL 60439, USA
rhu@anl.gov, fanning@anl.gov

Abstract

Large uncertainties still exist in the treatment of wire-spacers and drag models for momentum transfer in current lumped parameter models. To improve the hydraulic modeling of wire-wrap spacer in a rod bundle, a three-dimensional momentum source term that spirals around each rod has been developed. The momentum source model that accounts for the wire geometry is derived from momentum conservation and is dependent on local velocity profiles. Simulations of both 7-pin and 37-pin bundle configurations have been completed using the commercial CFD code STAR-CCM+ to simulate the wire-wrapped pin bundle as a bare bundle with extra momentum sources. The calculated inter-subchannel cross flow velocities match very well in comparisons between bare-bundle and wire-wrapped bundle cases. It has been confirmed that the momentum source model works well if its affecting region is accurately imposed. The validity of the model is further verified by mesh and parameter sensitivity studies.

1. Introduction

Modeling the flow in the analysis of wire-wrapped rod bundles is still a challenging problem. Large uncertainties lies in the treatment of wire-spacers and drag models in the momentum transfer of current low-resolution (lumped parameter) models. Some traditional subchannel codes, such as SAS4A/SASSYS-1[1] and SUPERENERGY-2[2], treat the wire effects as solely enhancement of turbulent mixing but ignore the directional cross flow between subchannels. Others, such as COBRA-4[3], ASFRE[4], and MATRA-LMR-FB[5], apply “forcing function” type models to account for the diversion flow but are limited in their applications to certain validated conditions (flow regime, channel geometry, or operating conditions), and rely on complex coefficients, which were derived from fitting certain sets of experimental data.

Recently, Computational Fluid Dynamics (CFD) simulations of wire-wrapped rod bundles have received extensive interest. This includes the work[6-7] preceding this work, as well as the work of Hamman and Berry[8], Gajapathy et al.[9], and Natesan et al.[10] who used RANS-based simulations to study geometries ranging from 7-pin to 217-pin configurations. However, the CFD simulations are still limited in their capability to characterize long-term transients or large system simulations. A multi-resolution approach is thus being pursued at Argonne National Laboratory to investigate the thermal-hydraulic behavior in wire-wrapped fuel pin bundles. Within the multi-resolution framework, high-resolution spectral LES methods are used to improve turbulence models for coarser resolution RANS based methods, and in turn, RANS simulations can be used to improve or extend correlations used in traditional sub-channel tools or coupled with the existing tools to model the whole plant behavior while resolving the details of important components.[11]

In this work, a three-dimensional momentum source term that spirals around each rod is introduced to characterize the wire-wrap effects on the hydraulics in the rod bundle. The wire-wrapped rod bundle can then be simulated using a bare-bundle geometry. This new modeling approach is being developed as part of the ongoing effort to pursue an intermediate-fidelity modeling capability for pin-bundle thermal-hydraulics and to fill the gap between RANS-based methods and traditional sub-channel methods.[12] A separate effort has been initiated for modeling the natural turbulent mixing due to velocity fluctuations.[13] The momentum source model was examined in both 7-pin and 37-pin configurations using the commercial CFD code STAR-CCM+[14]. Simulation results were compared between the reference wire-wrapped bundles and bare-bundles with extra momentum sources. The validity of the model is further confirmed by mesh and parameter sensitivity studies.

2. The Three-Dimensional Momentum Source Model

To account for the wire geometry, a three-dimensional momentum source (MS) model is derived from momentum conservation and is dependent on local velocity profiles. The momentum source is represented as a body force within the volume previously occupied by the wire-wrap. It is decomposed into three directions: normal to the wire and tangential to the pin n_n, along to the wire n_t, and normal to the pin and wire n_{pt}. The forces in the normal directions are to block the flow, while the force in the wire tangential direction is assumed to introduce additional friction:

$$\vec{f} = \vec{f}_n + \vec{f}_t + \vec{f}_{pn} \tag{1}$$

The Navier-Stokes momentum conservation equation for an incompressible fluid is considered:

$$\rho \frac{D\vec{v}}{Dt} = -\nabla p + \mu \nabla^2 \vec{v} + \vec{f} \tag{2}$$

In the wire normal direction,

$$\frac{Dv_n}{Dt} = \frac{\partial v_n}{\partial t} + v_n \frac{\partial v_n}{\partial n_n} + v_t \frac{\partial v_n}{\partial n_t} + v_{pn} \frac{\partial v_n}{\partial n_{pn}} \tag{3}$$

Assuming that the introduced body force is the dominant contributor to change the momentum of the fluid in the wire normal direction and neglecting the time-dependent term, we can obtain

$$f_n = (\rho v_n \frac{\partial v_n}{\partial n_n} + \rho v_t \frac{\partial v_n}{\partial n_t} + \rho v_{pn} \frac{\partial v_n}{\partial n_{pn}}) \cdot (-\vec{n}_n) \tag{4}$$

where

$\vec{n}_n = [\cos\varphi \cdot \cos(\theta - \pi/2), \cos\varphi \cdot \sin(\theta - \pi/2), \cos\varphi]$, wire normal direction;

$\vec{n}_t = [\sin\varphi \cdot \cos(\theta + \pi/2), \sin\varphi \cdot \sin(\theta + \pi/2), \cos\varphi]$, wire tangential direction;

$\vec{n}_{pn} = [\cos\theta, \sin\theta, 0]$, direction normal to both the pin and the wire.

The above normal vectors and the angles, $\theta = 2\pi z / H$ and $\varphi = a\tan(\pi(D + d_w)/H)$ are shown in **Figure 1**, where D is the pin diameter, d_w is the wire wrap diameter, and H is the wire wrap lead length. The velocity vectors are then $v_n = V \cdot \vec{n}_n$; $v_t = V \cdot \vec{n}_n$; $v_{pn} = V \cdot \vec{n}_{pn}$.

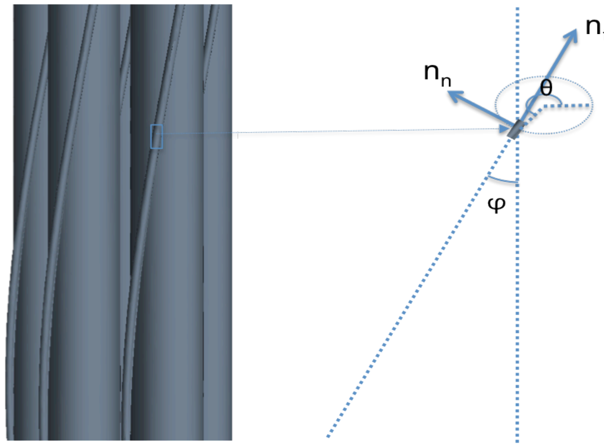

Figure 1: Geometry of the wire-wrapped pin bundle

Given the $[x, y, z]$ cell coordinates, the body force will be applied only to the region previously occupied by the wire: $d = \sqrt{(x - x_w)^2 + (y - y_w)^2} \le r_w = d_w/2$, where the coordinate of the center of the wire, $[x_w, y_w, z_w]$, relative to the center of the bottom surface of the pin are

$$\begin{cases} x_w = (R + r_w)\cos(t) \\ y_w = (R + r_w)\sin(t) \\ z_w = \dfrac{H}{2\pi} \cdot t \end{cases} \quad (5)$$

It is seen from Eq. (3) that the introduced force should be dependent on local velocity gradient caused by the existence of the wire. Considered examining the developed M.S. model first with a CFD software STAR-CCM+ and due to its limitation, i.e. only cell center velocity is available, the velocity gradients were assumed proportional to the cell center velocity in the normal directions. Set $\partial v_n/\partial n_n = Cv_n/d_w$, $\partial v_n/\partial n_t = Cv_n/(d_w/\cos\varphi)$, and $\partial v_n/\partial n_{pn} = Cv_n/d_w$, we obtain:

$$f_n = \frac{C\rho v_n (v_n + v_t \cos\varphi + v_{pn})}{d_w} \cdot (-\vec{n}_n), \quad (6)$$

where C is a multiplication coefficient. Since the fluid cannot flow through the wire, the velocity gradient should be large enough to block the flow in the directions normal to the wire. Thus, C should be larger than two, as illustrated in **Figure 3**.

Similarly, we can obtain

$$f_{pn} = \frac{C\rho v_{pn} (v_n + v_t \cos\varphi + v_{pn})}{d_w} \cdot (-\vec{n}_{pn}). \quad (7)$$

For the force in the wire tangential direction, a general form of friction force is assumed:

$$f_t = \frac{f_{fr} \rho v_t^2}{2d_w} \cdot (-\vec{n}_t), \quad (8)$$

in which f_{fr} is the friction factor. For simplicity, Blasius-McAdams correlation [15] for tube flow is used in this work. Later, the effects of the tangential force on flow distribution and pressure drop will be discussed.

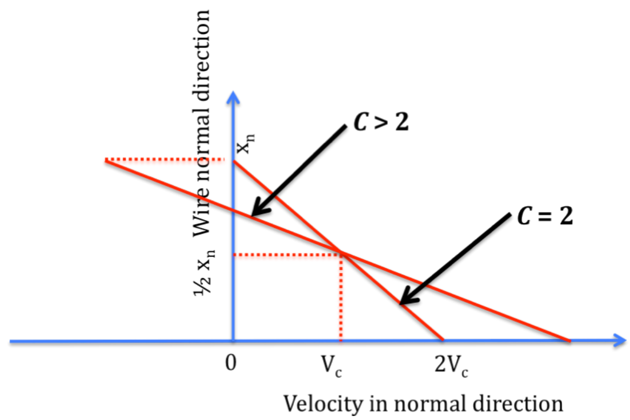

Figure 3: Illustration of minimum velocity gradient using velocity at cell center

3. 7-pin Bundle Simulations

The momentum source model was first examined in a 7-pin bundle configuration using the commercial CFD software STAR-CCM+, Star-CCM+ supports the use of generic polyhedral mesh elements, greatly simplifying the generation of computational meshes for complex geometries. All simulations presented herein are steady state RANS-based simulations using realizable k-ε turbulence model and the two-layer all-y+ wall formulation[14]. The SIMPLE predictor-corrector algorithm was used. Evaluations of sensitivities of predictions for 7-pin wire-wrapped fuel assemblies to computational mesh density, RANS turbulence model formulation, boundary flow conditioning, and comparisons to Large Eddy Simulations (LES) have been previously discussed in references [6] and [7]. It is confirmed that RANS-based simulations can provide acceptably accurate hydrodynamic predictions in the wire-wrapped bundle geometry. Several meshes were applied in the simulations of 7-pin wire-wrapped bundle, and good mesh convergence has been achieved. Although it is not perfect suitable in this exercise, the Grid Convergence Index (GCI) proposed by Roache[16], is calculated as a reference of the grid refinement error estimation. The calculated GCI is only 0.09 for the average cross flow velocity for a inner subchannel plane at the mid-span, which indicates high-quality CFD simulations.

Hydrodynamics inside a bare bundle is simulated to examine the impact of the momentum source model in which additional momentum sources were applied as described above. In STAR-CCM+, only cell centroids (coordinates at geometric center) are known. Thus, if the cell centroid is inside the wire, the whole cell is considered to be inside the momentum source affecting region. To obtain an accurate MS affecting region, an in-place interface for the wire surface was added in the STAR-CCM+ model, as shown in Figure 5. Later, the effects of this modeling will be examined.

The predicted lateral flow velocity distribution at the span outlet is shown in Figure 7, along with that of the wire-wrapped bundle case. The cross-flow distribution and magnitude are very similar for the two cases, except the abnormal high cross flow rate in the upstream of the wire and the high bouncing cross flow away from the wire, which is underestimated in the bare bundle with momentum source case. To facilitate the comparison between different simulations, average cross-flow velocities (normalized to the inlet velocity) were calculated as a function of axial position along four groups of inter-subchannel cut planes shown in Figure 9. Each cut plane occurs in six locations within the pin bundle, with each location shifted by 1/6th of the wire-wrap lead length. Matching locations will have similar hydraulic characteristics.

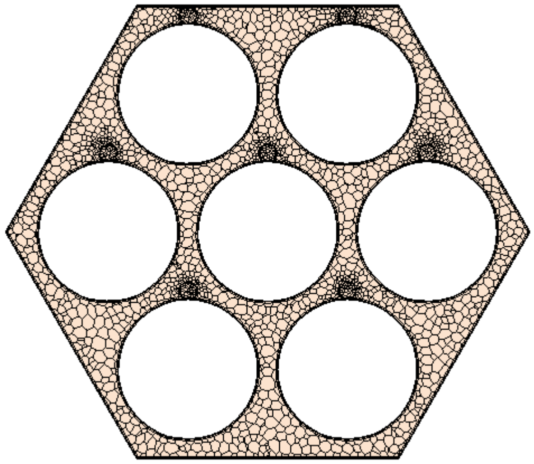

Figure 5: Mesh of a 7-pin bare bundle, wire surface conserved

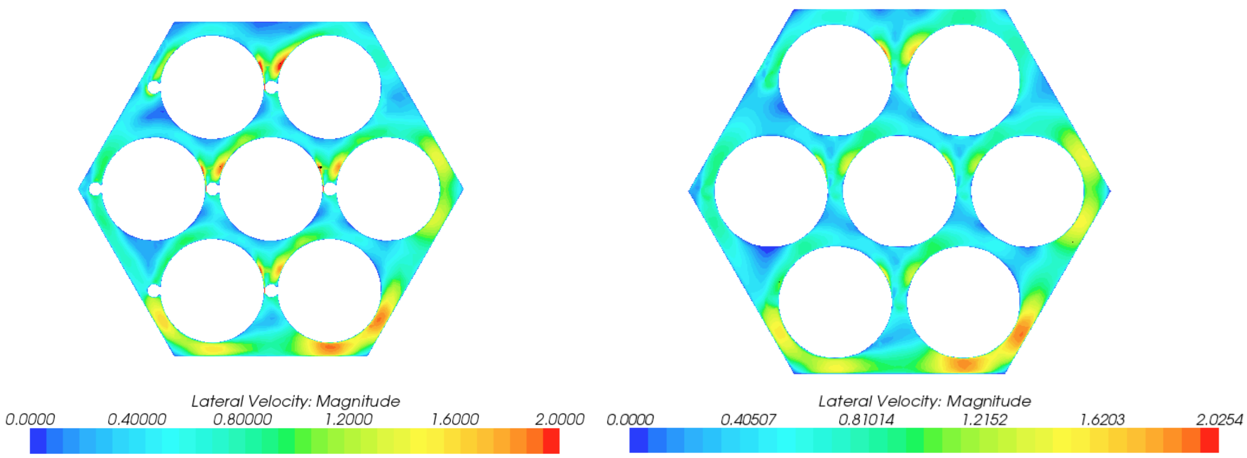

(a) Wire-wrapped bundle (b) Bare bundle with momentum source

Figure 7: Lateral velocity distributions at the mid-span plane in 7-pin bundles

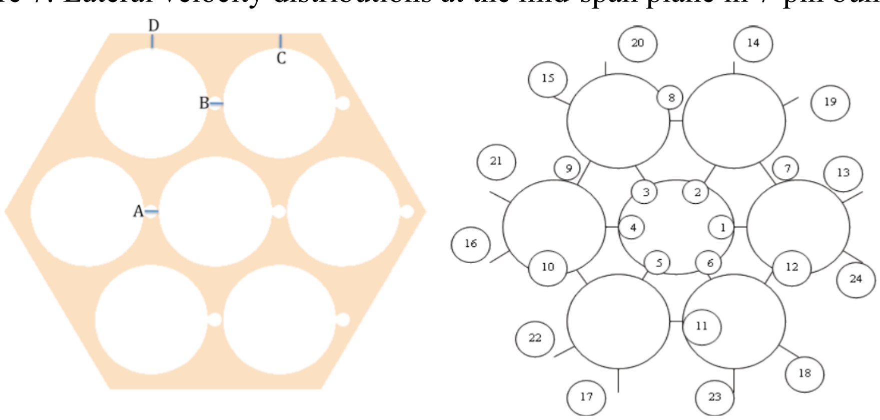

Figure 9: Geometry of the 7-pin wire-wrapped pin bundle; cut lines indicate planes and plane groups used for cross-flow comparisons (group A: plane 1-6; group B: plane 7-12; group C: plane 13-18; group D: plane 19-24.)

For the wire-wrapped pin bundle, the cross flow velocity distributions for planes in group A are shown in **Figure 11**. Almost identical profiles are obtained. If shifting them to the same phase, they will overlap each other. The same symmetry exists in the other groups, as well as in the plane groups in the bare bundle case. The results of these inter-subchannel cross-flow velocities for different plane groups (after shifting and averaging) are shown in Figure 13 for the wire-wrapped and bare-bundle cases. Very similar cross-flow velocities are found for all four types of plane groups, indicating that the proposed momentum source model is adequate for representing the wire-wrap effects on introducing swirl flow around the fuel pins. It is interesting to find that the sudden changes of the cross flow rates due to the wire-wrap sweep through the planes were also slightly reproduced by the new momentum source model. Sinus distributions are found for all four groups, but the inner-planes (A and B) are subject to two incidents where the wire-wrap sweeps through the planes, while at the outer planes (C and D) this happens once. At the inner planes, the coolant could flow both counter-clockwise (positive cross velocity) and clockwise (negative cross velocity) with symmetry. However, a strong counter-clockwise flow occurs in the outer planes.

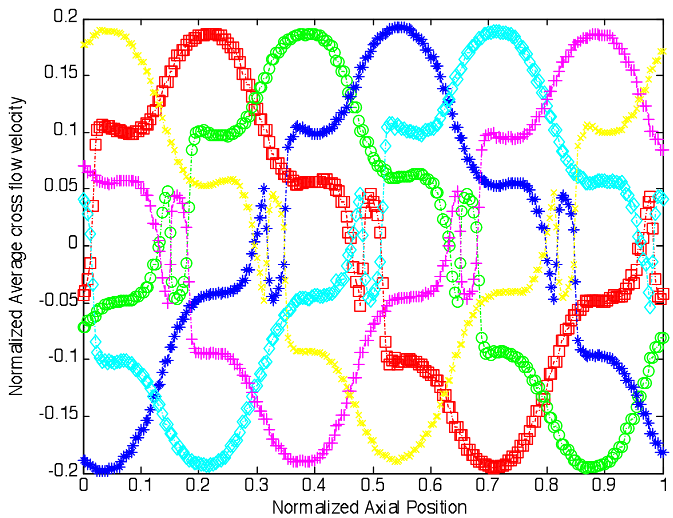

Figure 11: Cross flow velocity distributions for planes in group A, wire-wrapped bundle

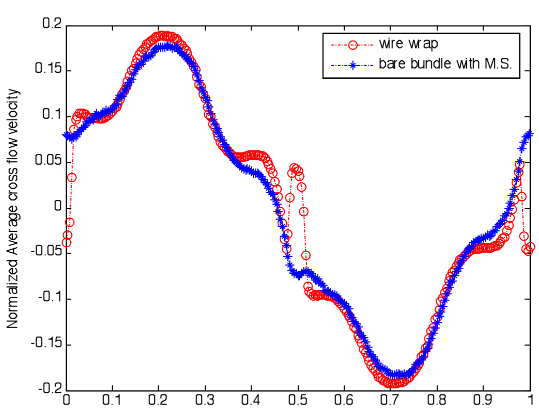

(a) Plane Group A

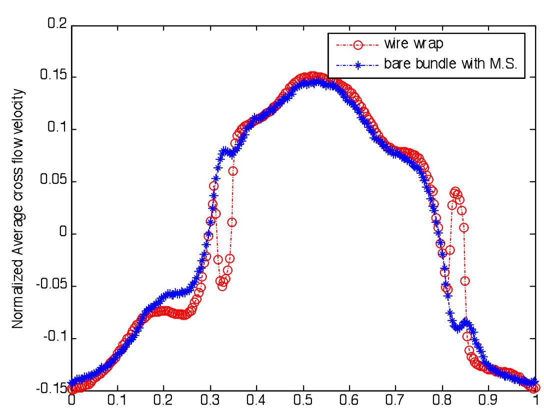

(b) Plane Group B

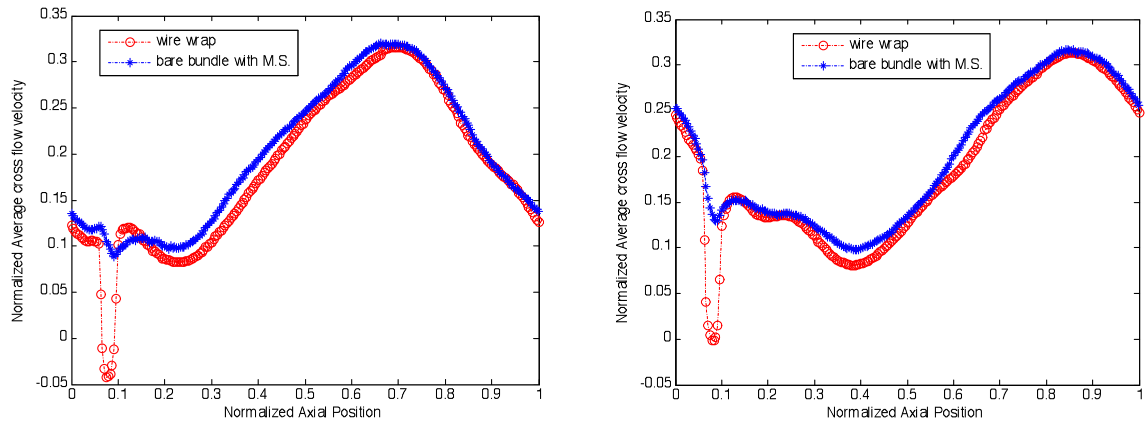

(c) Plane Group C (d) Plane Group D

Figure 13: Comparison of inter-subchannel cross flow velocities

4. Mesh and Parameter Sensitivity Studies in 7-pin Bundle

Additional simulations were conducted to examine the mesh and parameter effects of the momentum source model.

4.1 Mesh effects

A mesh sensitivity study was conducted by reducing the mesh cell number while conserving the wire surface. The cell number was reduced from two million (2,007,358 fine mesh) to 800K (807,581, coarse mesh 1) and then to 470K (470132, coarse mesh 2). Predicted cross-flow velocities are very similar among the different meshes. This is shown in Figure 15 for cross flow velocities at plane A. It has been concluded that if the wire outer-surface is conserved, the inter-subchannel cross flow rate is only weakly sensitive to the cell number.

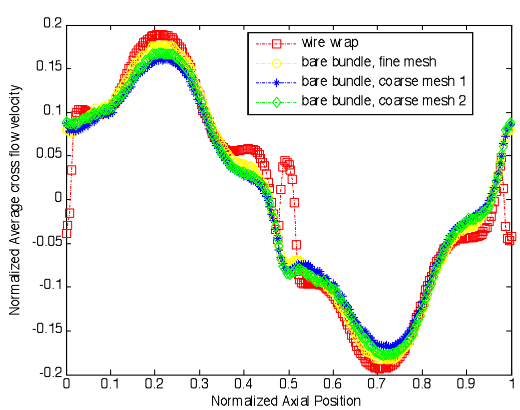

Figure 15: Cross flow velocity at inner planes, effects of mesh cell number

4.2 The effect of the tangential force

As discussion in Section 2, a force is introduced in the wire tangential direction to simulate the friction effects by the wire-wrap. It is of interest to investigate its effect on the cross-flow rates and pressure drop since it is modelled with a simple friction correlation.

A new simulation without the wire tangential force was conducted and compared with the full momentum source model. The inter-subchannel cross-flow velocities are shown in Figure 17, and the pressure drops are shown in Table 1. It is seen in Figure 17 that the force in the wire tangential direction only has minor effects on reducing cross flow rates. More significant effects are observed that contribute to pressure drop. Pressure drop reduces from 15.76 to 14.79 kPa when the tangential force is excluded.

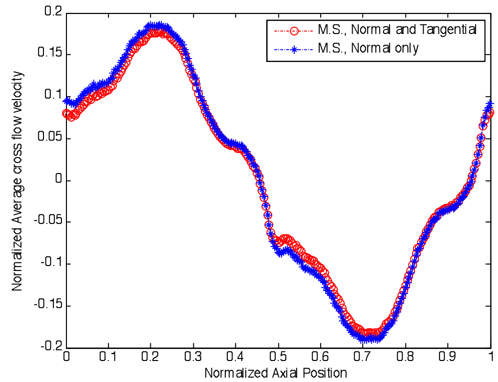

Figure 17: Cross flow velocity at inner planes, tangential force effect

Table 1: Pressure drop comparison among various momentum source models

Case	Wire-wrapped bundle	B.B. with M.S.	B.B. with M.S., without tangential force
Pressure drop (kPa)	15.61	15.76	14.79

4.3 Velocity effects

The MS model was derived from the N-S equations with very few assumptions, with the goal to be flow regime independent and to cover a wide range of operating conditions. Several different operating conditions were considered to evaluate the MS model with respect to flow regime.

The velocity effects on the amplitudes of the cross flow were first examined with the wire-wrapped bundle. Flow in the 7-pin wire-wrapped bundle at four different Reynolds numbers (56000, 28000, 5600, 1120) were simulated in STAR-CCM+, representing normal operating condition (turbulent flow), reduced turbulent flow, laminar-turbulent transition flow, and laminar flow conditions respectively. It should be noted that the laminar flow model was used for the Re = 1120 case, and the realizable *k-ε* turbulence model and the two-layer all-y+ wall formulation were applied to the other cases. The modeling choice of the laminar flow and laminar-turbulent transition flow conditions were verified with a comparative study of three models: laminar flow model, v2f *k-ε* model, and realizable k-ε model.

For the laminar flow case (Re = 1120), it was found that the predictions of the normalized cross flow velocities from the v2f *k-ε* model are consistent with the results from the laminar flow model, and the resulting turbulent kinetic energy is negligible. Thus, the flow is in laminar regime, and the standard realizable *k-ε* two-layer model should not be used. However, the realizable *k-ε* turbulent model, rather than the v2f model, should be used for laminar-turbulent transition flow case (Re = 5600) because: 1) the v2f model resulted in higher turbulent kinetic energy although it was intended for flow with small turbulence; and 2) the v2f model did not converge as well as the realizable *k-ε* two-layer model.

The resulting cross flow velocities in the wire-wrapped bundle cases were normalized and are shown in Figure 19. The cross flow velocities of the bare bundle with MS cases are compared with the results of the wire-wrapped bundle cases. Similar distributions were found for all different flow conditions, indicating that the normalized cross flow is dominantly dependent on the bundle geometry, not the flow regime. For most flow regimes, the results confirm that the cross flow velocities match well between the two modeling approaches, indicating that the MS model is valid for a wide range of operating conditions without adjusting any modeling parameters. However, the model did not work as well under laminar flow conditions. Nonetheless, it should not be an opposing factor for the application of the model, since during low flow conditions, energy exchange due to the cross flow is likely to be negligible comparing to conduction. Thus, the accuracy of the cross flow prediction is not expected to be critical to reactor safety. This issue will be revisited once an intermediate-fidelity method is established.

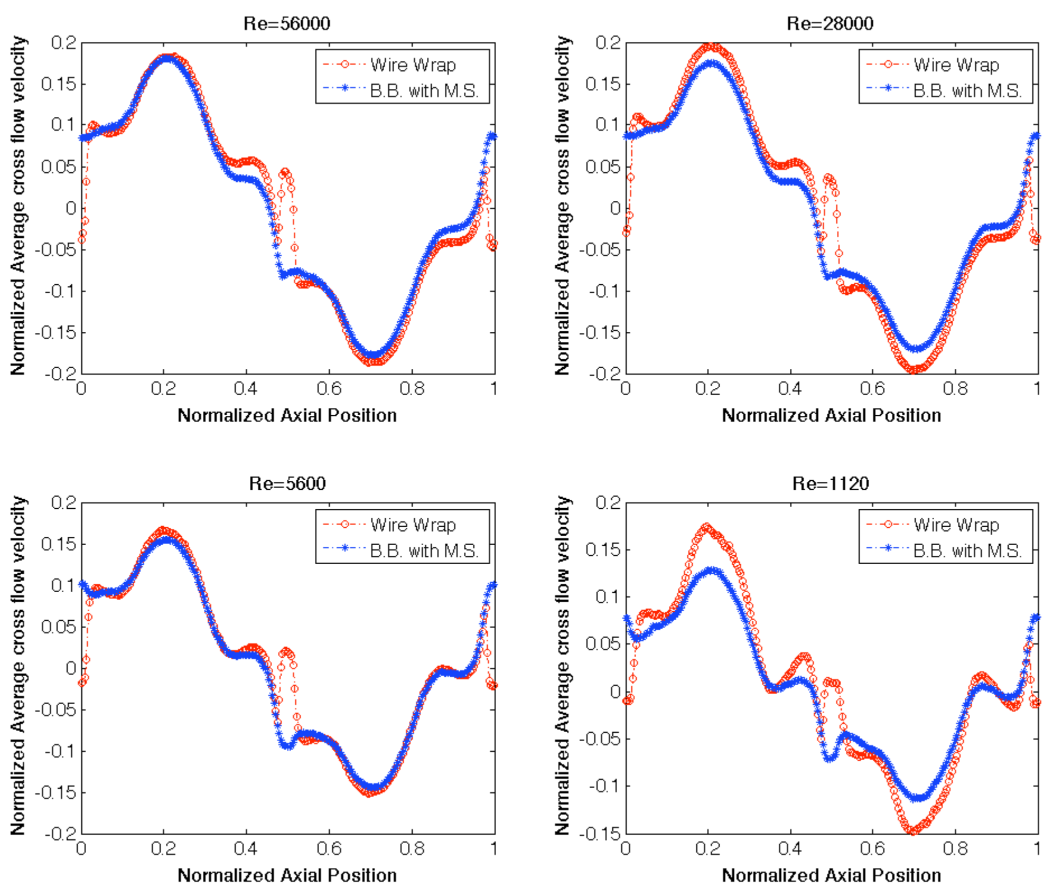

Figure 19: Cross flow velocities in wire-wrapped and B.B. with M.S. cases, velocity effects

5. 37-pin Bundle Simulations

To further examine the validity of the momentum source model described in Section 2, it is applied to a larger 37-pin bundle. For comparison, both the wire-wrapped pin bundle and the bare bundle with momentum source were simulated. The same models and boundary conditions used in the 7-pin bundle are applied.

A relatively coarse polyhedral mesh was used for the 37-pin wire-wrapped bundle, as shown in Figure 21. Again, average cross-flow velocities (normalized to the inlet velocity) were calculated as a function of axial position along the inter-subchannel planes for different types of plane groups shown in Figure 21.

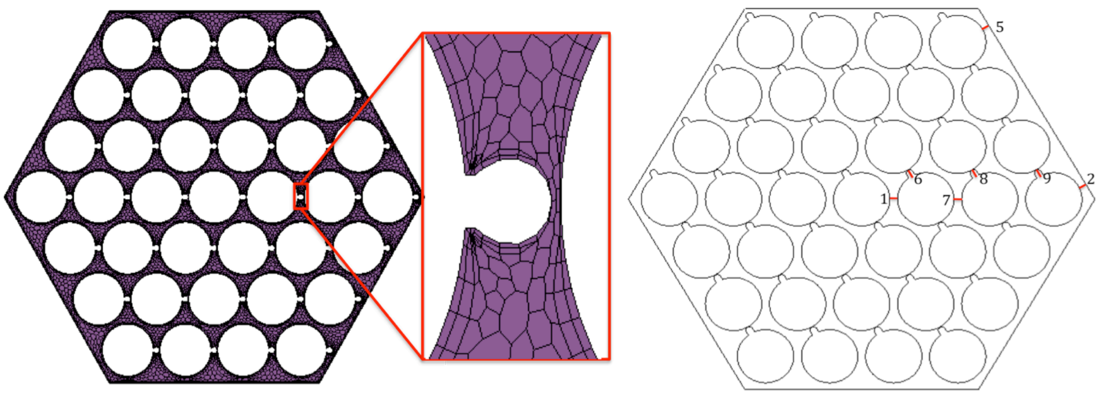

Figure 21: Mesh of a 37-pin wire-wrapped bundle in STAR-CCM+; cut lines indicate inter-subchannel plane groups

For the 37-pin bare bundle case, an in-place interface for the wire surface was also added in the STAR-CCM+ mesh to obtain an accurate MS affecting region, as shown in Figure 23. The inter-subchannel cross flow velocities for 4 typical plane groups are compared between the wire-wrapped and bare-bundle cases and is shown in Figure 25. The cross-flow distributions matched very well between the two cases for the four selected plane groups, indicating that the proposed momentum source model is also suitable for a 37-pin bundle.

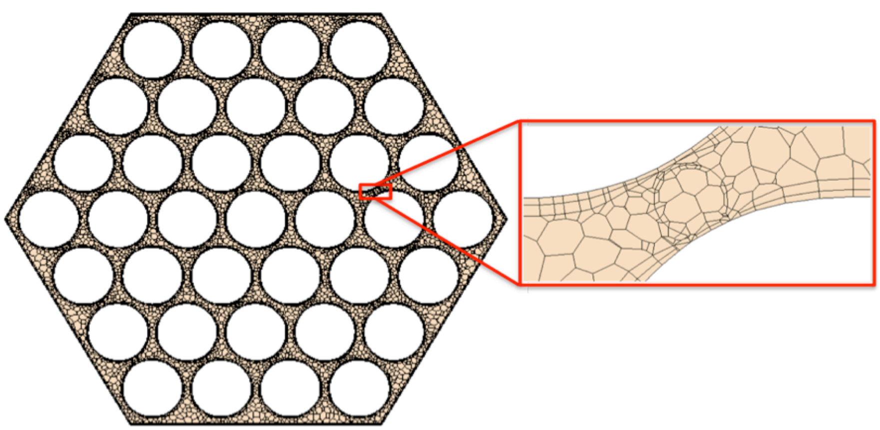

Figure 23: Mesh of a 37-pin bare bundle, wire surface conserved

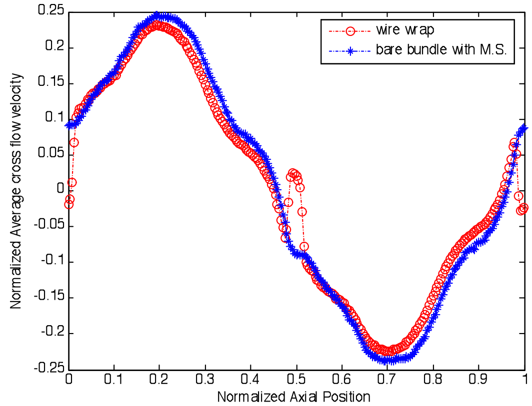

(a) Plane Group 1

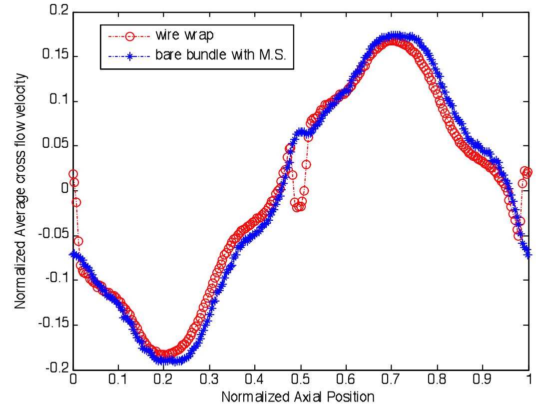

(b) Plane Group 7

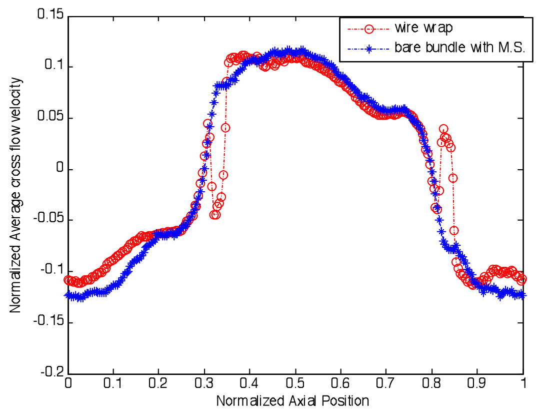

(c) Plane Group 9

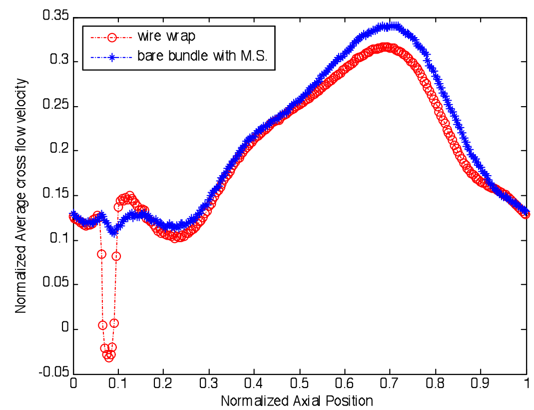

(d) Plane Group 2

Figure 25: Inter-subchannel cross flow velocities in 37-pin bundles

6. Conclusions

A three-dimensional momentum source model was developed to simulate the effects of wire-wrap spacer geometry on they hydrodynamic flow conditions in fuel pin bundles. The model was examined in both 7-pin and 37-pin bundle configurations using the commercial CFD code STAR-CCM+ to simulate both wire-wrapped and bare bundle geometries with momentum sources applied. It has been shown that the momentum source model works well if its affecting region is accurately imposed. The calculated inter-subchannel flow velocities match very well between the bare bundle and wire-wrapped bundle cases. The validity of the model is further confirmed by mesh and parameter sensitivity studies. Moreover, the model is valid among a wide range of operating conditions, from laminar-turbulent transition flow to high Reynolds number turbulent flow.

Because the momentum source model was derived from momentum conservation equations and depends only on local velocity profiles, it is expected that it can be applied to any wire-wrapped bundle geometries and any flow regimes. It is also expected that the modeling strategy can be applied to other conditions with complex or distorted geometry, such as flow in blocked channels. Further investigation will be focused on additional verification of the method and the implementation of the momentum source model into a fast-running intermediate-fidelity solver.

This will allow rapid, yet accurate simulations that can fill the gap between subchannel approaches and RANS-based CFD approaches.

Acknowledgements

The submitted manuscript has been created by UChicago Argonne, LLC, Operator of Argonne National Laboratory ("Argonne"). Argonne, a U.S. Department of Energy Office of Science laboratory, is operated under Contract No. DE-AC02-06CH11357. The U.S. Government retains for itself, and others acting on its behalf, a paid-up nonexclusive, irrevocable worldwide license in said article to reproduce, prepare derivative works, distribute copies to the public, and perform publicly and display publicly, by or on behalf of the Government.

References

[1] F. E. Dunn, D. Hahn, H. Jeong, K Ha, and J. E. Cahalan, "Whole Core Sub-Channel Analysis for LMR Passive Safety Analysis," 14th Pacific Basin Nuclear Conference, Honolulu, Hawaii, March 21-25, (2004).

[2] K.L. Basehore, N.E. Todreas, "SUPERENERGY-2: A Multiassembly Steady-State Computer Code for LMFBR Core Thermal-hydraulic Analysis," PNL-3379. Pacific Northwest Laboratory, Richland, WA, (1980).

[3] C.W. Stewart, C.L. Wheeler, R.J. Cena, et al., "COBRA-IV: the Model and the Method," BNWL-2214, Pacific Northwest Laboratory, (1979).

[4] H. Ninokata, A. Efthimiadis, N.E. Todreas, "Distributed resistance modeling of wire-wrapped rod bundles," *Nucl. Eng. Des.* 104, 93–102, (1987).

[5] H.Y. Jeong, K. S. Ha, W.P Chang, et al., "Modeling of flow blockage in a liquid metal-cooled reactor subassembly with a subchannel analysis code," *Nucl. Technol.* 149 (1), 71–87,(2005).

[6] W.D. Pointer, P. Fischer, A. Siegel and J. Smith, "RANS-based CFD Simulations of Wire- Wrapped Fast Reactor Fuel Assemblies," *Proceedings of ICAPP '08*, Anaheim, CA (2008).

[7] W.D. Pointer, J.W. Thomas, T.H. Fanning, et al., "RANS-Based CFD Simulations of Sodium Fast Reactor Wire-Wrapped Pin Bundles," Proceedings of M&C 2009, Saratoga Springs, New York (2009).

[8] R. Gajapathy, et al., "A comparative CFD investigation of helical wire-wrapped 7, 19 and 37 fuel pin bundles and its extendibility to 217 pin bundle," Nuclear Engineering and Design, 239, 2279-2292, (2009).

[9] K. Natesan, et al., "Turbulent flow simulation in a wire-wrap rod bundle of an LMFBR," Nuclear Engineering and Design, 240, 1063-1072, (2010).

[10] K.D. Hamman and R.A. Berry, "A CFD simulation process for fast reactor fuel assemblies," Nuclear Engineering and Design, 240(9), 2304-2312, (2010).

[11] T.H. Fanning, W.D. Pointer, and J.W. Thomas, "Multi-Resolution Modeling of Subassembly Pin Bundles for Advanced Fast Reactor Safety Simulations," *Proceedings of M&C 2009*, Saratoga Springs, New York (2009).

[12] R. Hu and T.H. Fanning, "Intermediate-Resolution Method for Thermal-Hydraulics Modeling of a Wire-Wrapped Pin Bundle," *Transaction of American Nuclear Society*, 103, 1003-1005, (2010).

[13] R. Hu and T.H. Fanning, "On the Modeling of Natural Turbulent Mixing in Wire-wrapped Rod Bundles," 2011 American Nuclear Society Annual Meeting, Hollywood, Florida, (2011).

[14] CD-adapco Group, "STAR-CCM+ User Manual v5.09," Melville, NY (2010).

[15] N.E. Todreas and M.S. Kazimi, "Nuclear System I, Thermal Hydraulic Fundamentals", Hemisphere Publishing Corporation, (1990).

[16] P.J. Roache, "Perspective: A Method for Uniform Reporting of Grid Refinement Studies", *Journal of Fluids Engineering*, Vol. 116, 405, (1994).